Instability of Ekman Flow at large Taylor Number

By MELVIN E. STERN,

Woods Hole Oceanographic Institution, Woods Hole, Massachusetts

(Manuscript received February 25, revised version August 22, 1960)

Abstract

A liquid of mean depth H is rotating at constant angular velocity (ω) inside a cylindrical annulus whose radial width is large compared to H and small compared to the mean radius. An equilibrium Ekman flow is then produced inside the boundaries by (for example) symmetrically forcing liquid into the annulus at the outer rim and removing the same quantity at the inner circumference. In response to the radial pressure gradient a geostrophic azimuthal velocity (U) is established above the inflowing viscous boundary layer; the latter extending to a characteristic height $h_E = (\nu/\omega)^{1/2}$ above the bottom surface of the annulus. This is a study of the shearing instability of an Ekman flow whose components are uniform in both horizontal directions.

We first discuss the anticipated similarities and differences of the stability of this "rotational" boundary layer and their counterparts in hydrodynamical flows which have no Coriolis force. Thus we note that the available kinetic energy in the boundary layer of the mean Ekman flow can be released by "pure-boundary" modes whose characteristic dimensions are of order h_E and whose onset condition only depends on a boundary layer Reynolds number $R = Uh_E\nu^{-1}$. This paper establishes the theoretical possibility of a qualitatively different energy releasing process, apparently confined to gyroscopic boundary layers, by "body-boundary" modes and suggests that for certain values of the Taylor number ($E = \omega H^2\nu^{-1}$) these may occur at lower Reynolds numbers than the pure boundary species. The energetic picture of this instability is as follows: Pressure fluctuations in the mean boundary layer, whose radial wavelength is much larger than h_E but much smaller than H and whose azimuthal wavelength is much larger than H, are partially (quasi-hydrostatically) transmitted vertically where they are accompanied by quasi-geostrophic azimuthal components of perturbation velocity and ageostrophic radial components. The coupling of this interior component with the boundary component of the perturbation influences the energy which is transferred to the latter from the *radial* (i.e. cross-isobaric) component of the mean field, and more than compensates for the burden of driving the perturbation against the stabilizing viscous forces in the interior of the fluid. Perhaps the most noteworthy aspect of these modes is that they can transport mean energy and momentum from the deep interior into the boundary, thereby making it available for further dissipation or to replenish the mean radial energy. The pure boundary modes, on the other hand, can only alter the geostrophic momentum in the interior by producing horizontal convergences of the mean flow in the friction layer.

We have used two slowly "converging" asymptotic expansions to obtain solutions of the characteristic value problem and have supplemented these results with error estimates to indicate the quantitative limitations in the range of physical interest. For large values of the Taylor number a disturbance of fixed horizontal wavelength will be unstable for values of the Reynolds number occurring in discrete ranges which are separated by other ranges in which the disturbance transfers energy *to* the mean flow. These unstable ranges or "scales" correspond to the set of eigenfunctions having different vertical structure. On the other hand for fixed supercritical Reynolds number there is a preferred radial wavelength in the n^{th} scale which is given by $2\pi m_n^{-1}E^{1/4}h_E$, where m_n approaches a numerical constant as $E\to\infty$. The corresponding minimum Reynolds number for the marginal stability of the n^{th} eigenfunction is $R_n = \varkappa_n E^{1/4}$, where $\varkappa_n$ is a numerical constant which only depends on the integer n, in the asymptotic limit $E\to\infty$. For the "largest scale of motion" $n = 1$, this asymptotic limit is easily reached under laboratory conditions (e.g. $E = 2{,}500$). Because of the limitations of the second asymptotic expansion we

can only estimate the numerical constants ($\varkappa_1$, m_1) as: $m_1 = 10^\circ$, $\varkappa_1 < 11$. Thus, for example, when $E = 2{,}500$ the Ekman flow should *not* be stable for Reynolds numbers as large as $8 \times 10'$. For larger values of E the Reynolds number which is necessary to destabilize the $n = 1$ scale increases. However smaller *scales* of motion (larger n) are preferred as E increases since it is found that $\varkappa_{n+1} < \varkappa_n$ in the asymptotic limit $E \to \infty$. The present theory is unable to determine that finite value of E when the second scale of motion becomes preferred over $n = 1$.

It is believed that a manifestation of this instability may be produced in the laboratory by causing a small decrease in the rate of rotation of a cylindrical vessel containing a shallow layer of water. Under certain conditions the decaying relative motion has the form of a time-modulated Ekman flow. By means of a permanganate solution placed in the boundary layer, the breakdown of this symmetric flow and the formation of thin rolls has been observed. We have also correlated experimental measures of the average rate of decay of relative angular momentum with a detailed laminar calculation (not included herein). For the converging Ekman flow, starting at a value of E of about 2,500, the measurements indicate a systematically greater mean decay rate than one would expect if the motion were laminar and symmetric. For the range of Reynolds numbers which were used in the experiment this critical point varied substantially less with changes in U (or R) than with changes in ω (or E). From these qualitative and quantitative observations we have concluded that the energy source for the instability is in the mean Ekman flow but that it cannot be entirely explained as a boundary layer phenomenon. It is suggested that the body-boundary modes discussed in the instability theory provide the mechanism for the increased transfer of angular momentum from the interior of the fluid to the lower boundary.

1. Introduction

In 1905 EKMAN (described in LAMB (1945) and numerous meteorological texts) published his theory of the equilibrium current which results from a balance of viscous, Coriolis, and ressure gradient forces in an attempt to describe the motion of a homogeneous ocean as the result of the stress exerted by the atmospheric winds. Although the insubstantial nature of the Austausch coefficient need no longer be dwelt upon, the physical process which the theory attempts to describe is undoubtedly of major importance for the transport process in the surface layers of both planetary fluids and to the general circulation problems to which they are ultimately coupled. Such flows as are predicted by Ekman's theory may, however, be realized in the laboratory by reducing the Reynolds number until laminar motion is obtained. Granting the relevance of laboratory models to the geophysical phenomenon we must pause to assay the utility of the problem of laminar instability, with which this paper deals, for the study of fully developed turbulence. Despite the gap in the non-linear scale which separates these two, several hydrodynamicists have worked in the belief that they are intimately coupled at least in those aspects pertaining to the transport problem. A recent theory of the mean velocity profile in turbulent pipe flow by MALKUS (1956) abandons detailed energy and momentum balance on the grounds that there are a multitude of solutions to the Navier-Stokes equations. The realized or most stable solution is conceived of as a discrete set of independent modes which draw their energy from, interact through, and consequently determine the mean field. This generalized eigenvalue problem and the quantification of the idea of "most stable solution" leads to a theory of the momentum transport.

The reader who is aware of the historical development of the theory of parallel flow instability will not expect the present paper to bring the Ekman problem to this state of development. The aim has been to explore the nature of the energy releasing process and to demonstrate by an asymptotic theory the possibility of a mode which is apparently confined to gyroscopic boundary layers. The mechanism which is discussed would appear to be of geophysical interest for the following reason. One usually conceives of the turbulence which originates at the boundary of the earth as effecting the flow in the interior of a statically stable atmosphere or ocean by means of large (synoptic) scale convergences in the boundary layer flow. This study establishes the physical basis for an additional and more direct type of coupling.

2. Statement of the problem

Fig. 1 is a schematic picture of a conceptually simple Ekman flow, and one which may be approximated in the laboratory. The section of water which is shown, is at some large distance from the axis of rotation of the smooth and rigid bottom surface. The homogeneous fluid with a free surface at height H is maintained in a horizontally uniform and steady flow relative to the bottom by means of the radial (γ') mass transport. Either this quantity or the geostrophic azimuthal current (U), which is

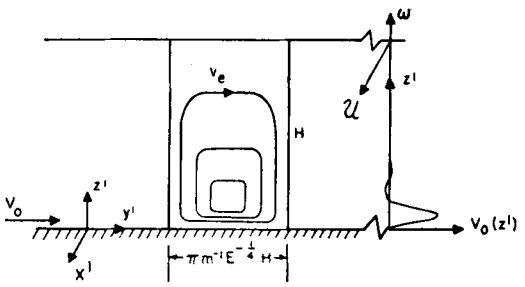

Figure 1. Schematic diagram of the mean Ekman flow and the body-boundary perturbation. The section is shown at a large radial distance from the axis of rotation (ω). V_0 is the "radial" (y') or cross isobar component of the undisturbed current. U is the amplitude of the azimuthal (x') component at or near the free surface. The radial half-wavelength of the perturbation is $\pi HE^{-1/4}m^{-1}$ where m is an order unity wave number, H is the height of the free surface and E is the Taylor number. v_e denotes the radial disturbance velocity in the interior of the fluid and the vertical concentration of the streamlines at the rigid bottom illustrates the boundary component of the mode.

produced by the hydrostatic transmission of the radial pressure gradient to the free surface, may be regarded as a primary known quantity in the analysis of the stability of this laminar Ekman flow.

Since the mean field is independent of the horizontal coordinates the non-linear terms in the equations of motion vanish and we can obtain an exact solution of the equations of motion involving a balance of viscous, Coriolis, and pressure gradient forces (e.g. Lamb sec. 334 a). This solution for the mean field is only a function of the vertical coordinate z', and shows that the ageostrophic motion is concentrated in a viscous boundary layer whose thickness is of order $h_E = (\nu/\omega)^{1/2}$ where ω is the rotation rate and ν is the kinematic molecular viscosity. Dimensional considerations of the Navier-Stokes equations with h_E as the unit of length, ω^{-1} as the unit of time and U as the unit of velocity lead to the conclusion that the instability of this flow can only[1] depend on a boundary layer Reynolds number ($R = U(\nu/\omega)^{1/2}\nu^{-1}$) and an Ekman or Taylor number ($E = \omega H^2\nu^{-1}$) which measures the ratio of total depth of the fluid to the thickness of the boundary layer.

Since the basic field gradients are confined to the boundary layer, the source of energy for a growing disturbance, or at least one of infinitesimal amplitude, must be in this region. There is then a tendency to classify the stability problem with other boundary layer shear flows. In the flow over a flat plate (Blasius), for example, the experiments of SCHUBAUER and SKRAMSTAD (1947) indicate that the total depth is not a significant parameter in the instability as long as it is much greater than the laminar boundary layer thickness. The measured value of the critical boundary layer Reynolds number is above 400. We also cite the case of the stability of the three-dimensional boundary layer produced by a circular disc rotating with angular speed ω in an ambient atmosphere of viscosity ν. The boundary layer thickness for this centrifugal fan is also $(\nu/\omega)^{1/2}$. GREGORY, STUART and WALKER (1955, p. 190) cite a range of 550—680 for experimentally determined value of R_{bnd}. In both examples the preferred horizontal dimension is proportional to the boundary layer thickness. If the unstable modes for the Ekman profile are also confined to the boundary layer, then the criterion only depends on R but not E. The analytical problem is more complicated than other shear flow instabilities because the mean field is not a parallel flow, and in addition it has a unique type of structure which is related to the Coriolis force. Nevertheless, it is a reasonable presumption that the Ekman flow will be unstable to boundary-like perturbations at Reynolds numbers of the same order as in the case of the centrifugal fan.

Preliminary experiments, to be referred to in Section VIII, suggested that the Taylor number was also a significant parameter. If this be the case, then one must admit a class of modes which extend throughout the depth of the homogeneous fluid and which satisfy the boundary conditions at the upper surface. Considering that no kinetic energy is available to the perturbation in this interior region, we may well ask if it is not more economical for the disturbance to confine itself to the boundary. The following asymptotic theory suggests two partial answers to this question. One is

[1] In accord with the neglect of the horizontal variation of the basic current we neglect the variation in height of the free surface. More precisely we have assumed a rotational Froude ($F = U^2/gH$) number which is small compared to one. In this attempt to isolate the mechanism under discussion, we have also neglected the rim boundary currents as a source of instability.

that the coupling of the so-called interior and boundary components of the perturbation increases the transfer of energy to the latter from the *boundary* layer of the mean flow, and more than compensates for the burden of driving the interior component. Secondly, disturbances on this scale perform a function which the pure boundary modes cannot. They are able (in the finite amplitude stage) to transfer mean energy from the remote *interior* and make it available in the Ekman layer for further dissipation. At large Reynolds numbers both species may be present.

3. Qualitative Remarks on the Energetics

In order to motivate the unusual dimensionalization of the equations of motion and the subsequent asymptotic expansion in the Taylor number, we make the following preliminary remarks concerning the free dissipation rate of disturbances in a rotating fluid. By this we mean that the energy source which drives the mean relative motion in Fig. 1 is removed and the fluid is in solid rotation except for a small initial perturbation $\mathbf{V}'$, which decays in time (t') due to the action of molecular viscosity. A class of disturbances which retain their shape during this decay process (i.e. the characteristic functions) may be found by writing $\mathbf{V}'$ as $\exp[-\lambda' t' + 2\pi i y'/L_y]$ times a function of z', where Ly is the wavelength of the disturbance in the "radial" direction and λ' is the decay rate. Since the discussion has been simplified by only considering those modes which are independent of x', the decay rate will only be a function of (ω, ν, H, L_y). We assert that under certain conditions (to be determined) this eigenfunction has a boundary layer structure, which in fact is similar to the classical Ekman profile for a mean flow that is both steady and independent of the horizontal coordinates. It consists of interior components (u_e, v_e) which are independent of z'. The azimuthal velocity u_e is in quasi-geostrophic balance while the radial velocity v_e is associated with interior momentum changes $(2\omega)^{-1}\frac{\partial u_e}{\partial t'}$. Since the interior components of the mode cannot satisfy the no-slip condition at $z' = 0$ we must add a viscous boundary layer component (u_b, v_b) extending to a charactesritic height $h_E = (\nu/\omega)^{1/2}$ above the bottom surface. A vertical section of the total perturbation is schematically indicated in Fig. 1. Almost all of the perturbation kinetic energy is in the interior, while almost all of the dissipation is in the boundary layer. The latter region is almost in equilibrium during the decay process as the result of its pressure coupling with the interior component, which in turn decreases the local kinetic energy by inviscid (almost) radial displacements. The perturbation kinetic energy averaged over one wavelength is then of order $u_e^2 H$. Since the boundary layer amplitude is of the same order as u_e it follows that the viscous dissipation due to vertical shear is of order $\nu(h_E^{-2})u_e^2 h_E$. On the other hand, the rate of dissipation due to lateral shear, a body effect, is of order $\nu L_y^{-2} u_e^2 H$. These two dissipation rates are of the same order when $L_y \sim (Hh_E)^{1/2} = E^{1/4}h_E = E^{-1/4}H$. When L_y is of larger order of magnitude than $h_E E^{1/4}$ the interior viscous force is negligible. Since total dissipation must equal the rate of decrease of kinetic energy $\lambda' u_e^2 H \sim \nu u_e^2 h_E^{-1} + \nu L_y^{-2} u_e^2 H$. We therefore conclude that when L_y is of order $HE^{-1/4}$ (or greater), $\lambda'/\omega \sim \nu\omega^{-1}h_E^{-1}H^{-1} = E^{-1/2}$. *Thus the horizontal dimension of the mode may be much less than the vertical dimension and still have no influence on the dissipation rate*, a situation which is in marked contrast with the analogous problem in a non-rotating fluid of depth H where the decay rate increases as L_y^{-2} and is independent of H for $L_y \gg H$. (For a more rigorous justification of these conclusions see the remarks following eq. (21) in Sec. IV.)

Let us now return to the stability problem where the question is one of balance of transfer and dissipation of energy. Although the mean field will affect the shape of the characteristic function, perhaps the previously discussed relation between dissipation and horizontal wave-length will be qualitatively unaltered, i.e., the dissipation increases slowly as the radial length of the mode decreases. At the same time the vertical component of the perturbation velocity increases relative to the horizontal component, for reasons of mass continuity. We therefore expect a relative increase in the Reynolds stress, as the horizontal dimension decreases, and consequently an increase in the transfer of energy from (or to) the mean flow. The qualitative idea that the transfer increases more rapidly than dissipation and eventually

overtakes it at some wavelength of order $HE^{-1/4}$ is explored in a more formal fashion below.

4. Asymptotic expansion in the Taylor number

We therefore choose a unit of time $(\omega^{-1}E^{1/2})$ equal to the free viscous decay time of these modes whose horizontal dimensions are much larger than the Ekman depth. With a unit of length equal to H and a unit of velocity (U) equal to the magnitude of the basic geostrophic flow, the equations of motion for the growth of infinitesimal perturbations $(\mathbf{V}')$ are:

$$E^{-1/2}\frac{\partial \mathbf{V}'}{\partial t} - E^{-1}\nabla\,{}^2\mathbf{V}' + 2\hat{z}\times\mathbf{V}' + \\ + \varkappa E^{-f}(\mathbf{V}_0\cdot\nabla\,\mathbf{V}' + \mathbf{V}'\cdot\nabla\,\mathbf{V}_0) = -\nabla p' \quad (1)$$

$$\nabla\cdot\mathbf{V}' = 0 \qquad (2)$$

$$\varkappa \equiv \frac{U}{\omega H}E^f = RE^{(f-1/2)}$$

where $\varkappa$ is to be regarded as a new independent parameter in lieu of the Reynolds number, and the scaling parameter f is to be determined in such a manner that it leads to a consistent asymptotic expansion at large E. $\hat{z}$ is a unit vector along the axis of rotation, and $\nabla p'$ is the normalized pressure force. The Ekman depth is now $E^{-1/2}$, and the basic field may be denoted by $\mathbf{V}_0 = \mathbf{V}_0(zE^{1/2})$, having a component V_0 in the y direction which decreases to zero at large values of $zE^{1/2}$ and having a component $1 + U_0(zE^{1/2})$ which approaches unity.

Since these fields are independent of the horizontal coordinates the eigenfunctions of (1) will be sinusoidal functions of (x, y). Let us now introduce the following scaling transformations for the (x, y, z) components of the velocity $\mathbf{V}' = (u', v', w')$:

$$\{u', v', w', p'\} = \exp(\lambda t + iymE^{1/4} + ixlE^{-a})\times \\ \{u, v, wE^{-b}, pE^{-c}\}$$

The reason for the choice of the y scaling in the above equation should be apparent from the remarks in Sec. 2, and we are free to assign values to a, b, c, f which will lead to a simplification of the eigenvalue problem at large E. Since the amplitude in a linear perturbation problem is arbitrary we may take the amplitude of the interior azimuthal velocity component (u_e) as unity. If we assert that the y component of the pressure gradient is of the same order, then since m is defined to be independent of E, $c = 1/4$. For the balance of azimuthal (x) interior forces we have indicated in Sec. 3 the importance of the Coriolis term proportional to v' and the inertial term proportional to $\left(\frac{\partial u'}{\partial t}\right)\omega^{-1}$. Since the latter is of order $E^{-1/2}$ in the interior then the amplitude of v' should be chosen of order $E^{-1/2}$ in the interior. The azimuthal scaling factor, $a = 1/4$, is then determined by requiring that the pressure gradient in the x direction is at most of the same order as the interior Coriolis force. In order to have a coupling between the boundary layer and the interior $\partial w'/\partial z$ in the latter region must be of the same order as the horizontal convergence, and this leads to $b = 1/4$.

The sole remaining scaling parameter is f and this will be chosen to make the transfer forces (like $E^{-f}w'\partial V_0/\partial z$) of the same order as the viscous force $(E^{-1}\nabla\,{}^2\mathbf{V}')$ in the boundary layer. With our previous choices the former is of order $E^{-f}E^{-1/4}E^{1/2}$ while the latter is of order $E^{-1}E^{+1}$, and therefore we take $f = 1/4$. In short, we introduce the transformation:

$$\{u', v', w', p'\} = \exp(\lambda t + iymE^{1/4} + \\ + ixlE^{-1/4})\{u, v, E^{-1/4}w, E^{-1/4}p\}$$

$$R = E^{1/4}\varkappa \qquad (3)$$

where λ, u, v, w, p are functions of the new and *independent* parameters $(\varkappa, E, l, m)$ and z. Equations (1) and (2) then become:

$$(a)\ \lambda E^{-1/2}v - E^{-1}\left(\frac{\partial^2}{\partial z^2} - m^2E^{1/2} - l^2E^{-1/2}\right)v + \\ + 2u + \varkappa\left[imV_0v + E^{-1/2}ilv(1 + U_0) + \right. \\ \left. + E^{-1/2}w\frac{\partial}{\partial z}V_0(zE^{1/2})\right] = -imp \qquad (4)$$

$$(b)\quad \lambda E^{-1/2}u - E^{-1}\left(\frac{\partial^2}{\partial z^2} - m^2E^{1/2} - l^2E^{-1/2}\right)u - $$
$$- 2v + \varkappa\left[imV_0u + E^{-1/2}il(1+U_0)u + \right. \qquad (4)$$
$$\left. + E^{-1/2}w\frac{\partial}{\partial z}U_0\right] = -ilpE^{-1/2}$$

$$(c)\quad \lambda E^{-1/2}w - E^{-1}\left(\frac{\partial^2}{\partial z^2} - m^2E^{1/2} - l^2E^{-1/2}\right)w +$$
$$+\varkappa[imV_0w + E^{-1/2}il(1+U_0)w] = -\frac{\partial p}{\partial z}$$

$$\frac{\partial w}{\partial z} = -E^{1/2}imv - ilu \qquad (5)$$

Equations (4) are of course equivalent to the original equations (1) and (2) since we have merely re-defined variables. Now however we introduce the assumption that for arbitrary but fixed values of $(\varkappa, l, m)$ the solution may be expanded in the small number $E^{-1/2}$ as follows:

$$u = u_{e0}(\varkappa, l, m) + E^{-1/2}u_{e1}(z, \varkappa, l, m) +$$
$$+ E^{-1}u^*_{e1}\left[(1-z)E^{1/2}\right] + \ldots. \qquad (6)$$
$$+ u_{b0}(\zeta, \varkappa, l, m) + E^{-1/2}u_{b1} + \ldots.$$

$$v = E^{-1/2}v_{e0}(\varkappa, l, m) + E^{-1}v_{e1}(z, \varkappa, l, m) + \ldots.$$
$$+ v_{b0}(\zeta, \varkappa, l, m) + E^{-1/2}v_{b1}(\zeta, \varkappa, l, m) + \ldots. \qquad (7)$$

$$\lambda = \lambda_0(\varkappa, l, m) + E^{-1/2}\lambda_1(\varkappa, l, m) + \ldots. \qquad (8)$$

$$\zeta \equiv zE^{1/2}$$

The subscript e denotes the body component of the perturbation, which describes the horizontal velocities in the region of vanishing mean field gradients. The leading term in (6) and (7) are independent of z; u_{e0} in fact being equal to 1 while the leading term for the radial interior velocity is of order $E^{-1/2}$, for reasons mentioned above. The boundary components of the mode, denoted by subscript b, are rapidly varying functions of z and which like U_0 and V_0 decrease to zero above the Ekman boundary layer. Their leading terms are of order unity since viscous forces are of the same order as inertial forces in the boundary layers. The last term (u^*_{e1}) in (6) identifies a boundary component at the free surface which is necessary, in high order iterations, to nullify the surface stress produced by the component u_{e1}. Substituting (6) and (7) in the continuity equation (5) and integrating gives the following expansion for the vertical velocity as a function of z or $\zeta \equiv zE^{1/2}$:

$$w = -iz(mv_{e0} + lu_{e0}) - iE^{-1/2}\int_0^z [mv_{e1} + lu_{e1}]dz$$
$$- im\int_0^\zeta v_{b0}(\zeta)\,d\zeta - iE^{-1/2}\int_0^\zeta (mv_{b1} + lu_{b0})\,d\zeta \qquad (9)$$

If the pressure perturbation at the undisturbed surface $(z=1)$ is denoted by p_{e0} then integration of the third equation of motion gives the following relation between pressure and velocity components:

$$p = p_{e0} + E^{-1/2}p_{e1}(z) + \ldots.$$
$$+ E^{-1/2}p_{b1}(\zeta) + \ldots. \qquad (10)$$

where

$$p_{e1}(z) = -\frac{i}{2}(\lambda_0 + m^2 + il\varkappa)(mv_{e0} + lu_{e0})(1-z^2) \qquad (11)$$

$$p_{b1}(\zeta) = -imv_{b0}(\zeta) + imv_{b0}(\zeta = E^{1/2})$$
$$+ \varkappa m^2\int_\zeta^{E^{1/2}} V_0(\zeta')\,d\zeta'\int_0^{\zeta'} v_b(\zeta'')\,d\zeta'' \qquad (12)$$

The velocity functions (u_e, v_e) and (u_b, v_b) are now determined by requiring that the former satisfy the dynamical equations (4a) and (4b) in the interior of the fluid $(z \gg E^{-1/2})$ where V_0 and $U_0 \to 0$, and by requiring that the latter satisfy the boundary layer equations formed by substracting the interior components from equations (4a) and (4b). When the coefficients of the terms containing the smallest power of $E^{-1/2}$ are set equal to zero, we get the following equations corresponding to (4a) and (4b) for the zero order interior components:

$$(a)\qquad 2u_{e0} + imp_{e0} = 0$$

$$(b)\quad \lambda_0 u_{e0} + m^2 u_{e0} - 2v_{e0} + il\varkappa u_{e0} + ilp_{e0} = 0 \qquad (13)$$

One then finds the zero-order boundary layer equations by substituting the expansions (6)—(12) in (4a)—(4b), cancelling terms corresponding to (13), and stretching the vertical coordinate by the transformation $z = \zeta E^{-1/2}$.

$$\begin{aligned} -v_{b0}''(\zeta) + 2u_{b0} + im\varkappa\left[V_0(\zeta)v_{b0} - \right. \\ \left. - V_0'\int_0^\zeta v_{b0}\,d\zeta\right] = 0 \\ -u_{b0}''(\zeta) - 2v_{b0} + im\varkappa\left[V_0(u_{b0}+u_{e0}) - \right. \\ \left. - U_0'\int_0^\zeta v_{b0}\,d\zeta\right] = 0 \end{aligned} \tag{14}$$

The sum of the two velocity components must vanish at $\zeta = 0$ and therefore the following zero order boundary condition must be satisfied:

$$\begin{aligned} u_{b0}(0) &= -u_{e0} \\ v_{b0}(0) &= 0 \end{aligned} \tag{15}$$

The two components of the perturbation are also coupled by the boundary condition on w at the upper surface. Thus when (9) is evaluated at $z = 1$ (or $\zeta = E^{1/2}$) and the result is set equal to zero we get (again to zero order):

$$mv_{e0} + lu_{e0} = -m\int_0^\infty v_{b0}\,d\zeta \tag{16}$$

Equations (13)—(16) are sufficient to specify the zero order eigenfunctions and growth rate once the amplitude of the perturbation is given. Since this quantity is arbitrary, we take $u_{e0} = 1$ for convenience and refer all perturbation amplitudes to this unit. Then when the pressure term is eliminated from equations (13) and v_{e0} is eliminated by (16) one gets the following expression for λ_0 in terms of the integrated boundary layer velocities:

$$\lambda_0 = -m^2 - il\varkappa - 2\int_0^\infty v_{b0}(\zeta)\,d\zeta \tag{17}$$

$$Re\lambda_0 = -m^2 + 2\,Re\phi(\infty, m\varkappa) \tag{18}$$

where $$\phi(\zeta, m\varkappa) \equiv -\int_0^\zeta v_{b0}(\zeta')\,d\zeta' \tag{19}$$

The new dependent variable ϕ is the vertical velocity due to horizontal convergence in the boundary layer and a single equation for it is obtained by combining the two equations in (14) as follows:

$$\begin{aligned} 2u_{b0} &= -\phi''' + im\varkappa(V_0\phi' - V_0'\phi) \\ -u_{b0}'' &+ 2\phi' + im\varkappa\left[V_0(u_{b0}+1) + U_0'\phi\right] = 0 \end{aligned} \tag{20}$$

or

$$\begin{aligned} \phi^{V} - im\varkappa\left[2V_0(\zeta)\phi''' + V_0'\phi'' - V_0''\phi'\right] + 4\phi' + \\ + im\varkappa\phi\frac{\partial}{\partial\zeta}(2U_0 + V_0'') - m^2\varkappa^2V_0(V_0\phi' - V_0'\phi) = \\ = -im\varkappa V_0 \end{aligned} \tag{21}$$

$$\phi(0) = \phi'(0) = \phi'(\infty) = 0$$

$$\phi'''(0) = 2$$

The asymptotic expansion in the Taylor number has reduced the characteristic value problem to the solution of equation (21) which contains only a single parameter $m\varkappa$. The important coupling with the body mode lies in the inhomogeneous boundary condition. The stability characteristics are obtained by evaluating this solution (ϕ) at $\zeta = \infty$ and substituting in (18). It is noted that when $m\varkappa = 0$ (no mean field) eqs. (14) have exactly the same form as the non-dimensional equations for an undisturbed Ekman boundary flow. Their integration is then readily accomplished and one finds $\phi(\infty, 0) = -1/2$ which corresponds to a decay factor $\exp -t(1+m^2)$. For $m \ll 1$ these "Ekman-like" modes have a decay rate independent of wave number, which agrees with the dimensional argument in Sec. 3.

It is a consequence of eq. (18) that if the real part of $\phi(\infty, m\varkappa)$ is greater than zero then the flow must be unstable to infinitesimal disturbances for sufficiently large Taylor numbers and sufficiently large Reynolds numbers. The marginal stability curve is obtained by setting (18) equal to zero and solving for $\varkappa$ as a function of $m\varkappa$, which then results in:

$$\lim_{E\to\infty}\quad \varkappa^2 = \frac{(m\varkappa)^2}{2Re\phi(\infty, m\varkappa)} \tag{22}$$

Notice that the wave number l does not appear in (22). This degeneracy means that as long as the azimuthal wavelength is much larger than the depth of the fluid there is no preference amongst all such infinitesimal disturbances.

Eq. (18) may also be interpreted as an energy balance for the interior motion, where the first term on the right is the viscous dissipation and the last term represents the energy which is transferred at the top of the boundary layer by the action of the perturbation pressure force. We have also obtained an expression for the first correction to this growth rate by setting the coefficients of the next largest power of $E^{-1/3}$ equal to zero. This is listed below for the purpose of obtaining the limits of validity of the foregoing expansion. Thus, correct to order E^{-1}

$$\lambda = -m^2 - il\varkappa + 2\phi(\infty, m\varkappa) + \frac{1}{E^{1/3}}\left[\frac{2}{3}m^2\phi^3 - \frac{2l}{m}\int_0^\infty u_{b0}\,d\zeta - 2\int_0^\infty v_{b1}\,d\zeta\right]$$

From the first term in the brackets we estimate that the zero order dissipation (m^2) is in error by a factor $\left[1 - \frac{2}{3}E^{-1/3}\,Re\phi^3\right]$, and since $Re\varphi = \frac{m^2}{2}$ at marginal stability the error factor is of order $\left[1 \pm \frac{1}{12}E^{-1/3}m^6\right]$. For $m \leq 1$ eq. (18) or (22) is quite adequate for any Taylor number of practical interest. For $m \gg 1$ (but independent of E) the Taylor numbers which are required by this expansion soon exceed laboratory possibilities.

5. Solution of the characteristic Equation (21) for $|m\varkappa| \gg 1$

The analytical complexity of (21) is such that we must again resort to asymptotic techniques. We could expand the solution as a power series in small values of $m\varkappa$ or, alternatively, in large values of $|m\varkappa|$. We choose the latter technique in order to demonstrate conclusively that $\phi(\infty, m\varkappa)$ is positive for some values of the parameter. We believe, however, that the vicinity $|m\varkappa| \sim 1$ which is beyond the reach of the following expansion, is of most interest for computing minimum critical R under laboratory conditions.

The mean Ekman boundary fields (U_0, V_0) are determined by the hydrostatic balance of viscous, Coriolis, and pressure gradient forces. Since ζ is measured in terms of h_E the appropriate equations are:

$$\frac{d}{d\zeta}(2U_0 + V_0'') = 0$$
$$-2V_0 + U_0'' = 0 \qquad (23)$$
$$0 = V_0(0) = 1 + U_0(0) = V_0(\infty) = U_0(\infty)$$

Using the first of these equations to eliminate U_0 in (21) we get the fifth order inhomogeneous equation

$$\phi^{V} - im\varkappa(2V_0\phi''' + V_0'\phi'' - V_0''\phi') + 4\phi' - m^2\varkappa^2V_0(V_0\phi' - V_0'\phi) = -im\varkappa V_0(\zeta) \qquad (24)$$

The additional relations in (23) also lead to a unique solution for V_0, viz. $V_0 = e^{-\zeta}\sin\zeta$. In adapting the asymptotic techniques that have been evolved for the Orr-Sommerfield equation (LIN, 1945) to the present problem, we will see that artificial singularities are introduced wherever $V_0(\zeta) = 0$. Since successive maxima and minima in the realized profile are in the ratio of the small number $e^{-\pi}$, let us first consider the formal problem of evaluating the integral $\phi(\infty, m\varkappa)$ for an arbitrary function $V_0(\zeta)$ which is positive for all values of ζ except at $\zeta = 0$ and $\zeta = \infty$, where $V_0(0) = V_0(\infty) = 0$, $V_0'(0) = 1$. It is anticipated that the desired integral property may be approximated by fitting some such positive definite V_0 to the realized profile $e^{-\zeta}\sin\zeta$ and that the associated error may be estimated from the r.m.s. departure of the two profiles. Although such smoothing may eliminate some modes, it is unlikely that the small ripple component could completely stabilize a mode which is found to be unstable by this approximation. In particular we shall consider the function:

$$V_0(\zeta) = e^{-\zeta}\sin\zeta, \qquad \zeta < \pi$$
$$V_0(\zeta) \to 0 \qquad \zeta \to \infty$$

with a suitably chosen smooth transition region at $\zeta = \pi$ whose width is of order $(m\varkappa)^{\circ}$ but much less than one.

The method of solution is as follows: Since the coefficients of (24) are analytic there will be five linear independent and analytic solutions. Asymptotic representations in $|m\varkappa| \gg 1$ for each of these may be found in the region $0 < \zeta < \pi$ and this will be referred to as the main boundary. These expansions will be seen to be singular at the end points, and one then looks for different representations valid in the vicinity of $\zeta = 0$ (called the lower boundary solution), and a set valid for $\zeta > \pi$ (called the upper boundary region). These must then be joined or otherwise identified to satisfy the end point conditions.

(a) *Main boundary solutions*

Equation (24) has one particular solution ϕ_p and five complementary solutions $\{\phi_1, \phi_2, \phi_3, \phi_4, \phi_5\}$. For $V_0(\zeta) \neq 0$ we may obtain two of these as asymptotic expansions of the form

$$\left\{\begin{matrix}\phi_1\\ \phi_p\end{matrix}\right\} = \frac{1}{m\varkappa} g_1(\zeta) + \frac{1}{(m\varkappa)^2} g_2(\zeta) + \ldots .$$

Substituting this in (24) and equating the coefficient of the highest power of $(m\varkappa)$ to zero gives

$$V_0[V_0 g_1'(\zeta) - V_0' g_1(\zeta)] = iV_0$$

$$g_1(\zeta) = \text{constant} \times V_0(\zeta) - iV_0 \int_{\zeta}^{1} \frac{d\zeta}{V_0^2} \qquad (25)$$

or

$$\phi_p \to -\frac{iV_0}{m\varkappa} \int_{\zeta}^{1} \frac{d\zeta}{V_0^2}$$

$$\phi_1 \to \text{constant} \times V_0(\zeta)$$

$$\text{As } |m\varkappa| \to \infty, \text{ for } 0 < \zeta < \pi \qquad (25\,a)$$

When ζ is small compared to unity (but still in the main boundary) $V_0 = e^{-\zeta} \sin \zeta \doteq \zeta$ and (25 a) becomes, $\phi_p \to \frac{-i}{m\varkappa}$, $\phi_1 \to \zeta$. Note however that $\phi_p''(\zeta)$ is singular at $\zeta = 0$.

Asymptotic forms for $\{\phi_2, \phi_3, \phi_4, \phi_5\}$ in the main boundary will be determined using the W.K.B. approach, in which it is asserted that there are rapidly (in ζ) varying complementary solutions of the type:

$$\phi = \exp\left[(m\varkappa)^{1/2} S(\zeta, m\varkappa)\right] \qquad (26)$$

When the inhomogeneous term from (24) is removed and (26) substituted therein one gets the following non-linear equation for the unknown function $S(\zeta, m\varkappa)$:

$$[(S')^5 - 2iV_0(S')^3 - V_0^2 S'] =$$
$$- (m\varkappa)^{-1/2}[10\,S''(S')^3 - 6iV_0 S''S' - iV_0'(S')^2 +$$
$$+ V_0 V_0'] - (m\varkappa)^{-1}[10 S'''(S')^2 + 15 S'(S'')^2 -$$
$$- 2iV_0 S''' - iV_0' S'' + iV_0'' S'] - \ldots -$$
$$- (m\varkappa)^{-2}(S^{V} + 4S') \qquad (27)$$

S is now expanded in a power series in terms of the small parameter $(m\varkappa)^{-1/2}$. Let:

$$S(\zeta, m\varkappa) = S_0(\zeta) + 0 + (m\varkappa)^{-1/2} S_1(\zeta) +$$
$$+ (m\varkappa)^{-3/2} \ldots \qquad (27\,a)$$

Then the leading term $S_0(\zeta)$ may be obtained by setting the right hand side of (27) equal to zero, thereby giving:

$$S_0'(\zeta)[(S_0')^2 - iV_0]^2 = 0 \qquad (28)$$

Eq. (28) is a fifth order algebraic equation in $\frac{dS_0}{d\zeta}$, whose solutions are:

$$S_{01} = \text{constant}$$

$$\{S_{02}, S_{03}, S_{04}, S_{05}\} = \pm i^{1/2} \int_0^{\zeta} V_0^{1/2}(\zeta)\, d\zeta +$$
$$+ \text{constant} \qquad (29)$$

The root $S_{01}' = 0$ corresponds to the slowly varying solution φ_1, as may be seen more clearly by obtaining the next approximation S_{11}. The two roots $\pm i^{1/2} V_0^{1/2}$ are degenerate roots of the quartic, which are resolved into four distinct roots in the next iteration of (27). When either of the two roots in (29) is substituted into the right hand side of (27) the term containing $(m\varkappa)^{-1/2}$ is found to vanish. If this were not the case, the first cor-

rection in (27a) would be $O(m\varkappa)^{-1/4}$ and not $O(m\varkappa)^{-1/3}$. Although formal substitution of (27a) into (27) then gives an intractable nonlinear *differential* equation for the first approximation $S_1'(\zeta)$, we know that the four rapidly varying eigenfunctions have the form:

$$\{\phi_2, \phi_3, \phi_4, \phi_5\} =$$

$$= \exp \pm [i^{1/2}(m\varkappa)^{1/2} \int_0^\zeta V_0^{1/2} d\zeta] \exp \pm [S_1(\zeta) + O(m\varkappa)^{-1/4}] \qquad (30)$$

If we content ourselves with the zero order solution, then

$$\phi \sim \text{constant} \times \exp [i^{1/2}(m\varkappa)^{1/2} \int_0^\zeta V_0^{1/2} d\zeta]$$
$$i^{1/2} = 2^{-1/2}(1+i) \text{ for } m\varkappa > 0 \qquad (31)$$

The symbol ($\sim$) denotes equality in the sense that the fractional departure of the logarithm of ϕ from the log of (31) approaches zero as $|m\varkappa| \to \infty$.

(b) *Upper boundary solutions* ($V_0 = 0$)

We have assumed that V_0 is zero for ζ somewhat greater than π. In this region the eigenfunctions must satisfy:

$$\phi^{V} + 4\phi' = 0 \qquad (32)$$

which is obtained by setting $V_0 = 0$ in (24). Eq. (32) has two solutions which decrease exponentially with height, *one which is constant*, and two which increase exponentially with ζ. The two of the main boundary solutions (presumably one from each of the degenerate solutions in (29)) which join to the exponentially increasing upper boundary solutions must be rejected to satisfy the condition $\phi'(\infty) = 0$; and the coefficients of the remaining functions must be chosen to satisfy:

$$\phi(0) = \phi'(0) = 0, \qquad \phi'''(0) = 2$$

after the proper join is made at $\zeta \doteq 0$.

(c) *Sub-boundary layer*

When the zero order roots (29) are substituted into the right hand side of (27) and $\zeta \to 0$ we note that the result becomes infinite. The dominant term is the one containing the fifth derivative of S. Using $V_0(\zeta) \doteq \zeta$, one finds that as ζ approaches zero:

$$(m\varkappa)^{-2} S_0^{V} \doteq -\frac{15}{16}(i)^{1/2}(m\varkappa)^{1/2}\zeta^{-7/2}$$

By comparing this with the left hand side of (27) as $\zeta \to 0$, it can be shown that (29) is a valid asymptotic approximation in the range $\zeta^3 \gg \varepsilon^3 \equiv |m\varkappa|^{-1}$. In order to find a representation of the eigenfunctions for values of ζ which are not large compared with ε we return to (24), stretch the vertical coordinate by the transformation $\zeta = \eta |m\varkappa|^{-1/3}$, and perform an asymptotic expansion by again letting $|m\varkappa| \to \infty$. With $V_0 \doteq |m\varkappa|^{-1/3}\eta$ this transformation of (24) leads to the following fifth order equation:

$$\left[\frac{d^5}{d\eta^5} - i\left(2\eta\frac{d^3}{d\eta^3} + \frac{d^2}{d\eta^2}\right) - \eta\left(\eta\frac{d}{d\eta} - 1\right)\right]\phi = = \left(\frac{-i}{m\varkappa}\right)\eta \qquad (33)$$

Since $\frac{d^3}{d\zeta^3}\phi = (m\varkappa)\frac{d^3\phi}{d\eta^3}$ we introduce $m\varkappa\phi = \psi$ and get the following equation for the sub-boundary layer:

$$\left[\frac{d^5}{d\eta^5} - i\left(2\eta\frac{d^3}{d\eta^3} + \frac{d^2}{d\eta^2}\right) - \eta\left(\eta\frac{d}{d\eta} - 1\right)\right]\psi = = -i\eta$$
$$\psi(0) = \psi'(0) = 0$$
$$\psi'''(0) = 2 \qquad (34)$$

Note that $\psi_p = -i$ and $\psi_1 = \text{constant} \times \eta$ are solutions to (34) which join on to ϕ_p and ϕ_1 in the main boundary. More important, we must require that the solution of (34) joins (31). Using a W. K. B. technique similar to a) above it is readily shown that

$$\psi \sim \text{constant} \times \exp\left[\frac{2}{3} i^{1/2}\eta^{3/2}\right]$$
$$i^{1/2} = 2^{-1/2}(1+i) \qquad (35)$$

is a logarithmically convergent asymptotic solution of (34) for $\eta \gg 1$. On the other hand for $\varepsilon \ll \zeta \ll 1$ eq. (31) becomes

$$\psi \sim \text{constant} \times \exp\left[\frac{2}{3} i^{1/4} (m\varkappa)^{1/4} \zeta^{3/4}\right] \quad (36)$$

which is identical to the sub-boundary solution (35). We can also obtain power series (in η) representations for ψ which are valid for $\eta \ll 1$.

d) *Piecing together*

In sections a), b), c) above we have obtained information about the form of the eigenfunction except in the vicinity of the two transitions points $\eta = 1$, $\zeta = \pi$. In order to join the functions in the various regions it would be necessary to obtain complete solutions of (34) over the whole range of η and to have the next approximation to the main boundary function. This we have been unable to do[2] and must therefore resort to an artifice which is consistent with the logarithmic accuracy of the above eigenfunctions.

We ask the following question. Is it possible to find a single functional representation which is analytic at all values of ζ and which:

(i) satisfies the boundary conditions

(ii) satisfies the differential equation in the main boundary by reducing to some linear combination of the zero order asymptotic solution in (31) for $\varepsilon \ll \zeta < \pi$

(iii) satisfies the upper boundary layer equation (32) for $\zeta > \pi$

(iv) satisfies the lower boundary equation (33) for $\eta \ll 1$ and for $\eta \gg 1$?

Although such a fit may be expected to describe the velocities in the transition zones $\zeta = \varepsilon$ and $\zeta = \pi$ with even less accuracy than in the main boundary, the size of these regions and the velocities in them are relatively small so that their contribution to $\int_0^\infty v_{b0}\, d\zeta$ will be negligible when $|m\varkappa| \gg 1$.

If the two zero order solutions in (30) are combined one obtains the function $\cosh\left[(m\varkappa)^{1/4} i^{1/4} \int_0^\zeta V_0^{1/4} d\zeta\right]$ which is much greater than unity in the main boundary. Accordingly the function

$$\phi = A\{1 - \cosh\left[(m\varkappa)^{1/4} i^{1/4} \int_0^\zeta V_0^{1/4} d\zeta\right] \quad (37)$$

reduces to (31) and is an asymptotic solution in this region. In contrast with the exponential function (31), eq. (37) is analytic at $\zeta = 0$ because in the vicinity of this point

$$\int_0^\zeta V_0^{1/4} d\zeta = \frac{2}{3}\zeta^{3/4}\left(1 - \frac{3}{10}\zeta + \ldots\right)$$

and

$$\cosh\left[(m\varkappa)^{1/4} i^{1/4} \int_0^\zeta V_0^{1/4} d\zeta\right] =$$

$$= 1 + \frac{i}{2}\left(\frac{2}{3}\right)^2 m\varkappa\zeta^3\left(1 - \frac{3}{10}\zeta\right)^2 + \ldots.$$

Therefore, if we choose $A = -\frac{3}{2im\varkappa}$ then $\phi'''(0) = 2$ and the function

$$\phi = \frac{3i}{2m\varkappa}\left[1 - \cosh\left\{(m\varkappa)^{1/4} i^{1/4} \int_0^\zeta V_0^{1/4} d\zeta\right\}\right] \quad (38)$$

satisfies the conditions (i), (ii) above. Furthermore for $\zeta \gg \pi$ eq. (38) approaches a constant and it therefore satisfies condition (iii). For $\varepsilon \ll \zeta \ll 1$ eq. (38) reduces to (36) or (35), while for $0 \le \zeta \ll \varepsilon$ it reduces to $-\frac{1}{2}\left(\frac{2}{3}\right) i\eta^3 + o(\eta^4)$ which is one of the polynomial solutions of (34). The function in (38) therefore satisfies conditions (iv) above.

An alternative interpretation of the sense in which (38) is an approximate solution is as follows: If it is substituted in the original differential equation (24) and the r.m.s. value of the resulting expression is divided by the r.m.s. value of one of the large terms in (24) (say ϕ^{V}), the result approaches zero as $(m\varkappa)^{-1}$. Thus the error is similar to the distortion which would be produced in the eigenfunction (satisfying the given boundary conditions) if an additional force were imposed on the physical system whose magnitude was small compared to the viscous force by a factor $(m\varkappa)^{-1}$.

[2] See RABENSTEIN (1958) for recent mathematical investigations of these difficult joining and identification problems.

To get the approximate value of $\int_0^\infty v_{b0}d\zeta$ we set $\zeta = \infty$ in (38) and obtain:

$$\phi(\infty, m\varkappa) \sim \frac{3i}{2m\varkappa}[1 - \cosh\{(m\varkappa)^{1/3} i^{1/3} \int_0^\infty V_0^{1/3} d\zeta\}] \tag{39}$$

This expression "converges" on the exact solution (for positive definite V_0) only in the sense that the percentage deviation in the logarithm approaches zero as $|m\varkappa| \to \infty$. Or stated otherwise we have:

$$\phi(\infty, m\varkappa) = -\frac{3i}{2m\varkappa}[1 - \cosh\{(m\varkappa)^{1/3} i^{1/3} \int_0^\infty V_0^{1/3} d\zeta + O(1)\}] \tag{39a}$$

When the real and imaginary parts of (39) are separated one obtains:

$$Re\,\phi(\infty, m\varkappa) \sim \frac{3}{2|m\varkappa|} \sinh\left(\gamma\left|\frac{m\varkappa}{2}\right|^{1/3}\right) \times \sin\gamma\left|\frac{m\varkappa}{2}\right|^{1/3} \tag{40}$$

$$Im\,\phi(\infty, m\varkappa) \sim \frac{3}{2m\varkappa}\left[1 - \cosh\left(\gamma\left|\frac{m\varkappa}{2}\right|^{1/3}\right) \times \cos\left(\gamma\left|\frac{m\varkappa}{2}\right|^{1/3}\right)\right] \tag{41}$$

$$\gamma \equiv \int_0^\infty V_0^{1/3} d\zeta$$

We note that (40) only depends on the mean-root value of the radial velocity profile and therefore is not very sensitive to detailed structure. The value of γ which is used in the subsequent calculation was approximated by taking:

$$\gamma = \int_0^\pi e^{-\zeta/2}(\sin\zeta)^{1/3} d\zeta \pm \int_\pi^{2\pi} e^{-\zeta/2}|\sin\zeta|^{1/3} d\zeta$$

$$\gamma = 1.1 \pm 0.04 \tag{42}$$

where the last term is an error estimate.

6. Marginal Stability and the Associated Transports

Eq. (39a) is an oscillatory function of $|m\varkappa|$ and therefore $Re\phi(\infty, m\varkappa)$ is certainly positive for some large values of the parameter. In view of this, we conclude from the growth rate formula (18) that cyclonic and anticyclonic Ekman flows are unstable to body-boundary modes at sufficiently large values of the Taylor number and the Reynolds number.

The asymptotic criterion for marginal stability is given by (22), and using the approximate relation (40) one then gets:

$$\varkappa^2 = \frac{1}{3} \frac{|m\varkappa|^3}{\sinh\left(\gamma\left|\frac{m\varkappa}{2}\right|^{1/3}\right) \sin\gamma\left|\frac{m\varkappa}{2}\right|^{1/3}} \tag{43}$$

$$\text{for } |m\varkappa| \gg 1$$

or

$$\frac{3}{8}\gamma^6\varkappa^2 = \frac{(\pi\mu)^6}{(\sinh\pi\mu)\sin\pi\mu} \tag{44}$$

where $$\pi\mu \equiv \gamma\left|\frac{m\varkappa}{2}\right|^{1/3}$$

Fig. 2 is a plot of (44) showing the first few of the infinite set of discrete branches which are associated with this equation. The ordinate is proportional to the value of $\varkappa = RE^{-1/4}$ which is necessary for the marginal stability of the mode with non-dimensional radial wave number m, and the abscissa is proportional to $|m\varkappa|^{1/3}$. Shown below this is the numerical value of $|m\varkappa|$ when $\gamma = 1$, which is approximately the value of (42). The dashed part of the first branch at small $m\varkappa$ indicates the failure of the asymptotic expansion, since the flow must be stable at $m\varkappa = 0$. A third axis ($E^{-1/3}$) has been drawn to emphasize the fact that the condition of marginal stability is determined by a surface in $\varkappa$, m, E space (in addition to the degenerate wave number k) and that the curves which have been drawn represent the intersection of that surface with the plane $E = \infty$. The heavy vertical lines $\varkappa m$ = constant (in Fig. 2) are asymptotes to the various branches I, II, III, ... and each unstable branch is separated from the next by stable regions in which the energy transfer is *from* the disturbance to the mean flow. If these

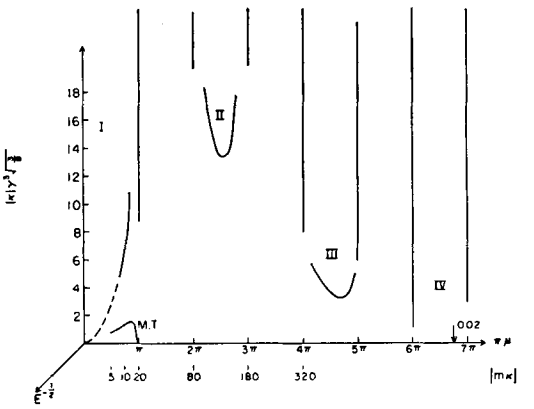

Figure 2. The section of the marginal stability surface for very large Taylor number showing parts of the four largest scales of motion. $\kappa = RE^{-1/4}$, $\gamma = 1.1$, $m =$ non-dimensional wave number. Only the minimum value for scale IV is indicated. The dashed part of I indicates its unreliability at values of $|m\kappa|$ which are not large compared to unity. The inset labeled *M.T.* (amplitude arbitrary) is the vertical momentum transport in the interior of the fluid as a function of $m\kappa$. The maximum point of this curve corresponds to the point which has been used in estimating an upper bound for R_1.

curves are plotted with m (rather than $m\kappa$) as abscissa and κ as ordinate then the asymptotes to the various branches will be the hyperbolae $\kappa = \frac{1}{m} \times$ constant. Consider the stability, for a given value of m, as κ (i.e. U) is increased. A line of constant m will intersect each branch at two values of κ, and the disturbance will grow when the value of κ lies between these two. As κ is increased further the energy transfer is reversed until the next branch is reached where there will be two more intersections, each corresponding to marginal stability. However the intersection of a constant m line with the $(n+1)^{\text{th}}$ branch occurs at larger values of κ (and $m\kappa$) than the corresponding intersection with the n^{th} branch, and therefore the associated eigenfunction will be a more rapidly oscillating function of ζ. This state of affairs is similar to the infinite set of discrete eigenfunctions which is found in the theory of thermal (Rayleigh) convection at marginal stability, and by analogy each branch in Fig. 2 will be referred to as a "scale" of motion. Each scale has a preferred disturbance, which in the asymptotic limit $E \to \infty$ is represented by the (relative) minimum point (κ_n, m_n). In this limit the minimum Reynolds number necessary for the onset of the n^{th} scale is given by $R_n = \kappa_n E^{1/4}$ and the preferred wavelength in centimeters is $L_y = 2\pi m_n^{-1} E^{-1/4} H = 2\pi m_n^{-1} E^{1/4} h_E$. In contrast with the case of thermal convection, where the least rapidly (in z) varying eigenfunction always occurs before (at lower Rayleigh number) the higher order eigenfunctions, Fig. 2 indicates that the preferred scale is a function of the Taylor number. Since $\lim_{E\to\infty} \kappa_{n+1} < \kappa_n$ (with the possible exception of $n = 1$) the $(n+1)^{\text{th}}$ scale should set in at a *lower* Reynolds number than the n_{th} scale, at sufficiently large Taylor number. It is therefore necessary to obtain the functional dependence of κ_n on E when $1 \ll E < (m_n^{12})$ (cf. remarks at end of sec. IV) in order to obtain a complete picture of the marginal stability.

The inadequacies of Fig. 2 in the region of practical interest may also be seen from the following calculations. First consider scale II for which the minimum is $\kappa_2 = 13.6$ at $m_2 = 5.8$. According to our error estimate in the Taylor number expansion this value of κ_2 can only be relied upon when $E^{1/4} \sim m_2^6 \sim 4 \times 10^4$, whereas a typical laboratory value is $E^{1/4} \sim 5 \times 10^1$. In scale I however the values of m are much closer to unity. For example the point $\mu = .8$ has an ordinate $\kappa = 11$ and corresponds to $m\kappa = 12.6$ when $\gamma = 1.1$. In this case $m = 1.1$ and m^6 is only 1.7 which is negligibly small compared to $E^{1/4} = 50$. Although we cannot resolve a minimum point for scale I because of the failure of the second asymptotic expansion at small $m\kappa$, it is believed that the value $m\kappa = 12.6$ is sufficiently large to justify using that point as an estimated *upper bound* for the minimum κ in scale I. Thus

$$\frac{R_1}{E^{1/4}} = \kappa_1 < 11 \tag{45}$$

Our discussion has been confined to the linear problem but it is of interest to compute the vertical transport of (angular) momentum by the Reynolds stress in the interior region of the fluid, in order to gain a picture of the tendency of the mean field modifications arising from the instability. Referring to Fig. 1 it is seen that the downward transport of cyclonic x') momentum is $-\overline{w'u'}$, where the

average is taken over one wavelength in both horizontal directions. For vertical distances much greater than the Ekman boundary thickness, the velocity components are found from (3) and (9) with $u_{e0} \equiv 1$, and are given by:

$$u' = Re\, e^{\delta}$$

$$w' = Re - iE^{-1/4}\left[m\int_0^{\infty} v_{b0}\, d\zeta + z\,(mv_{e0} + l)\right]e^{\delta}$$

$$\delta \equiv \lambda t + iymE^{1/4} + ixlE^{-1/4}.$$

Since $w'(1, x, y) = 0$ we find by virtue of (16)

$$w'(1 - \bar{z}, x, y) = Re\, i\bar{z}E^{-1/4} m\phi(\infty, m\varkappa)e^{\delta}$$

where $z + \bar{z} = 1$.

Therefore the downward transport of cyclonic momentum at a distance $\bar{z} < 1$ beneath the free surface is

$$-\overline{u'w'} = \frac{(\bar{z}m)}{2} Im\phi(\infty, m\varkappa)\, e^{2\tau Re\lambda}$$

$$= \frac{3}{4}\frac{\bar{z}E^{-1/4}}{\varkappa}\left[1 - \cosh\left(\left|\frac{m\varkappa}{2}\right|^{1/2}\gamma\right) \times \cos\left(\left|\frac{m\varkappa}{2}\right|^{1/2}\gamma\right)\right] e^{2\tau Re\lambda} \qquad (46)$$

in which the asymptotic expression (41) has been used. Therefore if $\cos\gamma\left|\frac{m\varkappa}{2}\right|^{1/2} = \cos\pi\mu$ is negative the downward transport of momentum has the same sign as $\varkappa$. Referring to fig. 2 or (44) it will be seen that the minimum points for scales II, III ... correspond to angles $\pi\mu$ which are in the second quadrant. When $\varkappa > 0$ (cyclonic rotation of the basic flow) the preferred infinitesimal disturbance transports cyclonic angular momentum downwards from the interior regions and tends to produce a uniform reduction of the mean momentum here. Similarly, when $\varkappa < 0$ the Reynolds stress produces a downward transport of anti-cyclonic momentum. In either case the preferred disturbance tends to transfer momentum down the mean gradient. It should be pointed out however that in each scale there are less favored disturbances for which $\cos\pi\mu$ is positive and which transport momentum up the mean gradient. In inset labeled M.T. in Fig. 2 is a plot of eq. (46) as a function of $m\varkappa$ for the largest scale of motion. Although the amplitude is arbitrary its sign is positive and there is a maximum in the vicinity of the point which has been chosen to estimate an upper bound for $\varkappa_1$. It is also of interest to compute the radial transport of momentum due to the correlation of u' and v' in the interior. The amplitude v_{e0} is obtained from (16) and $u_{e0} = 1$. One then computes $\overline{u'v'} = \frac{E^{-1/2}}{4}[2Re\phi(\infty, m\varkappa) - 2l/m] = \frac{E^{-1/2}}{4}\left(m^2 - \frac{2l}{m}\right)$ at marginal stability. This is positive for axial symmetric disturbances or for $2l < m^3$, and in these cases the growing disturbance tends to transport cyclonic angular momentum towards the center of rotation.

We should also like to know to what extent each of the two components (U_0, V_0) is responsible for driving the perturbation. This question is most readily answered from eq. (21), which is the boundary layer equation before the functional relation between U_0 and V_0 is introduced. Note that U_0 only appears in one term which subsequently vanishes by virtue of (23). However this term is also relatively small at large values of $m\varkappa$ and would be neglected in sec. 5 on that score. It is therefore the momentum terms which are associated with V_0 which are of importance in the boundary layer at large values of $m\varkappa$, and consequently it is the work done by the Reynolds stress on this radial component of mean velocity which balances the dissipation in the boundary layer and in the interior.

7. Summary of assumptions and conclusions

The model abstractions and mathematical approximations which were used in this theory are listed below.

i) The basic Ekman flow has no horizontal divergence and is only a function of the vertical coordinate. Such flows can only be approximated in the laboratory due to the circular geometry of the rotating vessel and the side walls. The influence of a basic gravitational stability has not been considered, although it is recognized that in the geophysical context this quantity may have a controlling influence on the scale height.

ii) The slope of the free surface which must accompany the rotation has been neglected in applying the boundary condition on the vertical velocity. This is a valid approximation if the rotational Froude number does not exceed unity.

iii) The pivotal approximation in this study is the boundary layer separation of the eigenmode and the subsequent expansion in the Taylor number. Since the associated error is of order $m^6E^{-1/2}$ this is quite adequate for the largest scale of motion ($m \sim 1$), when $E^{1/2} \gg 1$. However for the smaller scales (II, III . . .) the preferred value of m is much greater than unity and $E^{1/2}$ must therefore be much larger than m^6 in order that the asymptotic result be valid.

iv) The boundary layer equation for the eigenfunction which is obtained from this expansion (iii) is a function of only one parameter ($m\varkappa$). Slowly "converging" approximations for the necessary vertical integral of this function have been obtained using a W.K.B. approximation for the limiting case $|m\varkappa| \gg 1$. This is inadequate for computing growth rates at the long wave-length side of scale I, and does not give a resolution of the minimum critical $\varkappa$ for the largest scale of motion.

v) In connection with iv) the Ekman profile $V_0 = e^{-\zeta} \sin \zeta$ has been smoothed and the eigenvalue found for arbitrary positive definite V_0. Although it is possible that additional modes may be associated with the neglected ripple component in V_0 it is believed that the minimum critical Reynolds number will only be affected to the extent of the r.m.s. departure of the realized profile and that positive definite function which was chosen to fit it.

vi) We have only considered the growth of infinitesimal perturbations and leave unanswered the following question. Is it possible that modes of finite amplitude produce a momentum transport which alters the mean field in such a fashion that the disturbance becomes unstable at lower Reynolds number than a corresponding one of infinitesimal amplitude? It is worth pointing out that the linear theory of Poiseuille instability, which is much more accurate than this calculation, does not give quantitative agreement with observed minimum critical Reynolds numbers. There is reason to believe that finite amplitude effects are responsible for this discrepancy.

vii) We do not know the stability characteristics of the pure boundary modes (i.e. modes of the first species which were referred to in the Introduction). If these occur first, then we would have to know the subsequent modification of γ to determine the onset condition for the larger scale body-boundary modes (assuming a separability of the two stability problems on the basis of the difference in scales).

The following conclusions have been drawn from the theory:

i) A non-convergent Ekman boundary flow is unstable to body-boundary modes at sufficiently large values of the Taylor and Reynolds number. These draw their energy primarily from the cross-isobar component of the mean field and may be expected to produce a direct modification of the interior geostrophic flow depending on the difference of the Reynolds number and the critical R.

ii) The estimated upper bound for the minimum critical Reynolds number is given by

$$RE^{-1/4} = \varkappa_1 < 11$$

Thus for a typical laboratory value of $E = 2{,}500$ the Ekman flow should not be stable at Reynolds numbers as large as 80. It is conceivable that instability may set in at much lower values for reasons mentioned previously.

iii) The radial wavelength of the preferred disturbance which is associated with ii) is

$$L_y = 2\pi m_1^{-1} E^{1/4} h_E$$

where m_1 is a numerical constant which can only be estimated as $m_1 = 10°$. The azimuthal dimension of this disturbance should be much larger than the scale depth.

iv) At $\varkappa_1$ the disturbance with wave number m_1 is marginally stable while disturbances with slightly different wave numbers are damped. There are also (relative) minimum Reynolds numbers corresponding to the marginal stability of the higher order eigenfunctions. The preferred eigenfunction, or the smallest of the set of relative minimum Reynolds number, depends on the Taylor number. At sufficiently large E the $(n+1)^{\text{th}}$ scale is preferred over the nth scale. There may be certain critical values of E where two such disturbances, with

markedly different wavelengths, can be observed at the same minimum critical Reynolds number.

v) The relative magnitudes of the perturbation velocities in different regions may vary considerably, depending on the values of the Taylor and Reynolds numbers. The radial component near the free surface is smaller (by a factor of $E^{-1/3}$) than the velocities in the boundary layer, while the latter are large compared to the interior azimuthal velocities by order $|\phi(\infty, \varkappa m)|$.

8. Experimental Evidence

The author's interest in the preceding stability problem came from an earlier experimental study of the transient Ekman flow which is produced when a shallow cylindrical vessel of water is suddenly decelerated from one rotation rate to another. If the initial equilibrium rate ω is decreased by a small amount $\Delta\omega$, the fluid will rotate at a uniformly greater rate than the container, except at the bottom (and the rim) where a quasi-steady and convergent Ekman layer will be formed. Above this, for reasons of mass continuity, there is a weaker divergent radial flow which is responsible for the local decrease of angular momentum in the interior. If rotationally stable floats be placed on the free surface, their total relative angular deflection (Θ), during the readjustment process, is an inverse measure of the mean decay rate. These experimental quantities will be compared with values predicted from the Navier-Stokes equations on the basis of the assumption that the flow is always axi-symmetric and laminar. We would like to ascribe systematic departures in this comparison to an asymmetric instability, even though it is recognized that there are conceptual difficulties in defining stability for inherently transient mean fields.

The cylindrical tank which was used in these measurements had a radius (A) of 52 cm, and was centered and leveled on a rotating platform built by VON ARX (1952) for oceanographic model experiments. It was driven by a variable speed motor in the range $\Delta\omega/\omega = {}^1/_{20}$ to ${}^1/_3$ with most measurements in the vicinity of $\Delta\omega/\omega = {}^1/_{10}$ and $\omega = 1$ rad/sec. Fluctuations in motor speed of 1% were noted and this produces a 10 % uncertainty in the parameter $\Delta\omega/\omega$ at average conditions. However the period of these fluctuations is much smaller than the four—five minutes which occupy the entire decay process and therefore these fluctuations will be partially averaged out if one uses four—five minute averages of the initial and final motor speeds to compute $\Delta\omega$. This is believed to be the limiting factor in the uncertainty of the experimental data which is estimated to be less than 5 %. The bottom of the container was fitted with a glass plate and covered to a nominal depth of $H = 5$ cm (kept constant in all runs) with tap water. The temperature of the latter was only measured at the start and finish of a day's experiment and the viscosity was computed from the mean. Since the dissipation of total angular momentum depends on the square root of the viscosity the uncertainty in our measurements due to this factor is 0—3 %, less than or equal that due to the fluctuation in motor speed. After some trial, it was decided to use four ${}^1/_2''$ circular cardboard floats as an indicator of the relative angular deflection of the water near the free surface. These were tested before the experiment with regard to orbital stability and relative deflection, when the fluid and container were in solid rotation. In a time interval (4—5 minutes) corresponding to the length of each experimental measurement of Θ, no significant angular deflection could be detected. The four floats were initially set 90° apart, and their distance from the center of rotation ranged from $A/4$ to $3A/4$ with most measurements near mid-radius. A glass cover plate placed on top of the container isolated the surface of the fluid from the drag of the air in the room, and a grid ruled upon it served to measure the initial and final position of the floats. The average relative angular displacement was one revolution and the uncertainty in obtaining the coordinates is negligible.

The data so obtained was plotted in Figs. 3 and 4. The ordinate in these figures is essentially the total angular deflection per unit change of angular velocity, since for small values of $\Delta\omega/\omega$ the logarithmic ordinate becomes $-\Theta\left(\frac{\Delta\omega}{\omega}\right)^{-1}$. In this limit the abscissa reduces to $E^{1/3}(1 + F/4)$, where $F = \left(\frac{\omega^2 A^2}{gH}\right)$ is

the rotational Froude number. It therefore is essentially a measure of the mean rotation rate since H was held constant in the experiments. It is easy to show by integrating the linearized Navier-Stokes equations with respect to time that the relationship between these two limiting quantities is linear to the extent that $\Delta\omega/\omega$, $E^{-1/2}$ and H/A are much less than unity. Since $\Delta\omega$ could not be controlled by the nominal motor setting but had to be measured after the fact, we have extended this calculation to include larger values of $\Delta\omega/\omega$. The elaborate coordinates in Fig. 3 and Fig. 4 are an attempt to reduce the data so that they fall on a single curve, for all $\Delta\omega/\omega$. If the relative motion were laminar, then our points should all fall on the heavy straight line which, under present operating conditions, differs by no more than 1 % from an exact initial value solution of the Navier-Stokes equation. This calculation has not been included herein because it is long and not especially pertinent. It is based on a boundary layer expansion in $E^{-1/2}$ and includes finite amplitude effects, correct to order $(\Delta\omega/\omega)^3$, as well as the variation in the height of the free surface and the vertical velocities associated with the convergent flow.

Each plotted point in Figs. 3 and 4 is the average displacement of the four floats in a given run and the thin vertical line gives the extremes. The geometrical symbolism used in plotting the points reflects variations in R

$$\left(\text{multiply } \frac{\Delta\omega}{\omega}E^{1/2} \text{ by } A/H = 10 \text{ to get } R\right).$$

For relatively small values of E and all values of R the experimental points are, within observational error, in agreement with the straight line predicted by the symmetric theory. However, Fig. 3 shows a systematic departure from this line beginning at values of $E^{1/2}$ of about 50 (the maximum value of the rotational Froude number in these experiments was 1.6). All values of the Reynolds number are associated with a larger decay rate than one would expect if the motion were laminar, and there is less reproducibility and coherency of the points corresponding to fixed R. This increase in the average rate of dissipation is attributed to an "instability" in the "slow" decay of the laminar Ekman profile. The peculiar aspect of the transition zone (abscissa 50—55) in Fig. 3 is that the critical parameter appears to be the

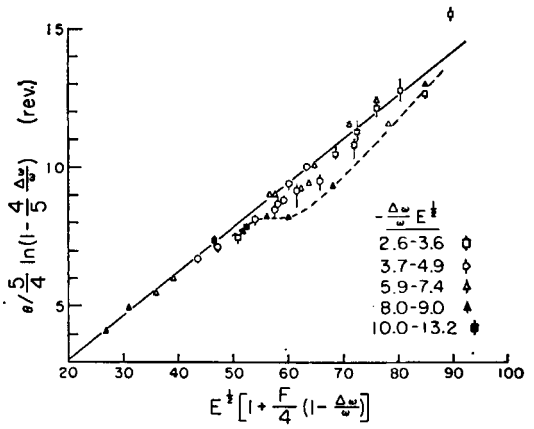

Figure 3. The average rate of decay of an Ekman flow produced by decreasing the rotation rate (ω) of a shallow cylinder by the amount $\Delta\omega \cdot \Theta$ is the total relative angular deflection (in revolutions) of floats placed on the free surface. $F = \frac{\omega^2 A^2}{gH}$ is the rotational Froude number. To get maximum boundary layer Reynolds number multiply figures in legend $\left(\frac{\Delta\omega}{\omega}E^{1/2}\right)$ by $A/H = 10$. Heavy straight line is theoretical computation of the decay assuming laminar mean motion. Thin vertical line through the experimental points indicates the extremes in the displacement of four surface floats and the broken curve is an envelope of the data (ln = log e).

Taylor number rather than the Reynolds number. The latter range from values of 40—130 in a small interval about $E^{1/2} = 50$. In Fig. 4 (anti-cyclonic relative motion) the data are in satisfactory agreement with the

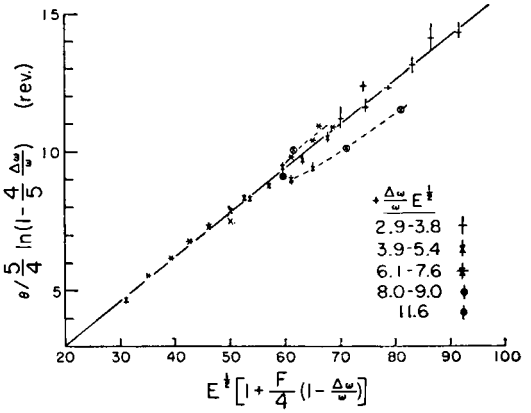

Figure 4. Same as Fig. 3 except $\Delta\omega > 0$. The relative motion is now anti-cyclonic and the Ekman boundary flow diverges from the center of rotation.

laminar theory to somewhat larger Taylor numbers. Above abscissa of 60 the dashed envelope of the experimental points indicates a departure from laminar decay but the data are inadequate to infer any systematic behavior.

In addition to these measurements, separate visual observations were also made to detect the instability. A thin layer of permanganate dye was diffused on the bottom of the rotating tank and concentrated as an annular ring near the circumference. When the rotation rate is suddenly decreased, this ring of dye converges towards the center of rotation with the Ekman boundary flow. During the first two revolutions after the change in motor speed the inside of the converging permanganate front retains its initial circular form. At this time, however, the circular front (located at radius $\frac{3A}{4}$ to $A/2$) begins to fold along about one-fourth of the circumference, as if there were an additional surge of fluid towards the center. Seconds later, roll striations appear with axis parallel to the fold, as was indicated by areas of varying dye concentration. These rolls then spread from this area and one may see the striations in many regions of the fluid in complex (but rather stationary) orientations of the axes. Considerable variation in the size of the small dimension of the roll have been detected in photographs (not included herein). These range in size from less than to much less than a centimeter while the large dimension of the roll has a wavelength of perhaps one-third the circumference. It has been reproduced many times[3] even in the region of Fig. 3 below abscissa of 50! I do not believe that the dye concentration was sufficient to introduce any extraneous effects in these qualitative observations. No systematic asymmetry was detected in the surface motion!

For the experimental conditions corresponding to Fig. 3, the following conclusions have been drawn. The quasi-steady Ekman motion which is produced by decelerations in the rotation rate of the container is "unstable" for certain values of the parameters. The dye observations indicate that the energy source for the disturbance is in the boundary layer of the mean flow. However the observed transition point (abscissa of 50 in Fig. 3) is much more sensitive to changes in ω than $\Delta\omega$ (or U), and therefore it cannot be entirely represented in terms of a boundary layer Reynolds number $R = U/(\nu\omega)^{-1/2}$. It is suggested that the Taylor number is an equally important non-dimensional parameter, and that the scale depth plays a role in the instability. The independent visual observations also suggest that the flow was unstable at abscissa less than 50. Therefore the transition which is detected by the quantitative measurement may mark the onset of a new scale of disturbance, which has a relatively larger influence on the mean field at these operating conditions. The dashed line, which is the envelope of the experimental data in Fig. 3, suggests a tendency towards stabilization as the value of the abscissa increases to 100. It would be interesting to see if a new transition is observed as the Taylor number is increased. Regarding the data for the anticyclonic flow (Fig. 4), I do not feel it is adequate to attempt to draw conclusions at large $E^{1/4}$ concerning the proposed instability.

It should be emphasized again that there are substantial differences between the theoretical model and the laboratory experiment. For reasons which have been mentioned a quantitative comparison of results cannot be made at this time. Whether or not there is any intimate connection in mechanism, I think the two studies are complementary in suggesting rather unexpected couplings between the friction boundary and the quasi-geostrophic flow in the interior of a rotating fluid.

Prof. A. ARONS and his students at Amherst College (1961, in press) have performed an experiment in which an Ekman flow is formed by forcing water into a rotating tank at the inner rim and letting the water level rise. They have informed me of axial symmetric instabilities which have a structural resemblance to those which are discussed in this theory and whose radial wavelength is proportional to $h_E E^{1/4}$. In the range of E from 1.5×10^3 to 2×10^4 they find a constant of proportionality $m = 3.0 \pm 20\ \%$. However, these instabilities are observed at critical R ranging from 1.5 to 3.4, considerably below the upper bound which has been estimated by this theory.

Dr. A. Faller of the Woods Hole Oceano-

[3] Similar disturbances have been seen in the large (20 foot) tank at Woods Hole. The depth of water was greater than in the above case while the basic rotation was about $^1/_6$ rad/sec.

graphic Institution is also experimenting with Ekman instability, in a geometry more like the one to which this theory pertains. I wish to acknowledge with gratitude the discussions in which his ideas and preliminary results were freely given. The work reported here has been supported by the Office of Naval Research (U.S.) under Contract Nonr 2196(00).

REFERENCES

ARONS, A., INGERSOLL and GREEN. Experimentally Observed Instability of a Laminar Ekman Flow in a Rotating Basin. *Tellus* (in press).

GREGORY, M., STUART, J. T. and WALKER, W. S., 1955. On the stability of three dimensional boundary layers, etc. *Phil. Trans. Roy. Soc.*, London, Vol. ***A248***, pp. 155—199.

LAMB, H., 1945. *Hydrodynamics*. Dover Publications, New York. Sixth Edition, p. 593.

LIN, C. C., 1945. On the stability of two dimensional parallel flows. Part I. *Quart. J. Applied Math.* Vol. **3**, pp. 117—142.

MALKUS, W. V. R., 1956. Outline of a theory of turbulent shear flow. *J. Fluid Mech.* Vol. **1**, pp. 521—539.

RABENSTEIN, A. L., 1958. Asymptotic solutions of, etc. *Arch. Rational Mech. and Analysis*, Vol. **1**, pp. 418—435.

SCHUBAUER, G. B. and SKRAMSTAD, H. K., 1947. Laminar Boundary Layer Oscillations and Transition on a Flat Plate. *J. Res. Nat. Bur. Stand.* **38**, pp. 251—292.

VON ARX, W. S., 1952. A laboratory study of the wind-driven ocean circulation. *Tellus* **4**, pp. 311—315.